

Formulation, Physicochemical Characterization, and in Vitro Bioefficacy Assessment of a Nanoemulsion-Based Delivery System of *Nigella sativa* Seed Oil for Enhanced Anti-Inflammatory and Antioxidant Activity

¹Senthil Rajan Dharmalingam, ²Mohd Mudassir Hussain, ³Amol Sambhaji Balsane*, ⁴Basu Venkateswara Reddy, ⁵Sharmila Mondal, ⁶Preeta Bose, ⁷Anuva Samanta, ⁸Priyanka Anand

¹Prof & HOD, Department of Pharmaceutics, Swamy Vivekananda college of Pharmacy, Tiruchengodu, Namakkal Dt, Tamil Nadu. 637205

²Professor and Principal, ISL Pharmacy College, Bandlaguda, Hyderabad.

³Lecturer, Pravara Rural College of Pharmacy Diploma, Loni, Rahata, Ahmednagar, Maharashtra. 413736

⁴Professor and Head, Department of Pharmaceutics, Sri.K.V.College of Pharmacy, Chikkaballapura, Karnataka. 562101

⁵⁶⁷Assistant Professor, Jis University, 81A Nilgunj Rd, Jagarata Pally, Deshpriya Nagar, Agarpara, Kolkata-, West Bengal. 700109

⁸Assistant Professor, Department of Pharmacy, Chandigarh Pharmacy College, Chandigarh Group of Colleges Jhanjeri, Mohali, Punjab, India. 140307

*Corresponding Author
Amol Sambhaji
Balsane*

Article History

Received: 14.10.2025

Revised: 06.11.2025

Accepted: 26.11.2025

Published: 16.12.2025

Abstract: This study aimed to develop and evaluate a nanoemulsion-based delivery system of *Nigella sativa* seed oil to enhance its anti-inflammatory and antioxidant activities. A series of formulations were prepared using Tween 80 and PEG 400 as surfactant-co-surfactant systems, and the most stable nanoemulsion (NE4) was selected following thermodynamic stability testing. The optimized formulation exhibited a nanoscale droplet size of 68.42 ± 1.85 nm, a narrow polydispersity index, and a zeta potential of -32.4 mV, indicating excellent physical stability. Physicochemical characterization confirmed high transparency, low viscosity, and efficient drug loading. The in vitro release study demonstrated a sustained drug release of 92.46% over 24 hours, fitting best with the Higuchi kinetic model. Biological evaluations revealed that NE4 significantly improved anti-inflammatory efficacy, with higher protein denaturation inhibition and RBC membrane stabilization compared to pure oil. Similarly, antioxidant assays—including DPPH, nitric oxide scavenging, and TBARS—showed substantially enhanced radical scavenging activity for NE4. Stability testing over 90 days indicated only minor variations in particle size and drug content, reinforcing the robustness of the formulation. Overall, the findings support the potential of nanoemulsion-based approaches to increase the therapeutic performance of *Nigella sativa* oil for inflammation and oxidative stress management.

Keywords: *Nigella sativa* • Nanoemulsion • Thymoquinone • Anti-inflammatory activity • Antioxidant activity

INTRODUCTION

Inflammation and oxidative stress represent two interconnected biological processes that play central roles in the pathogenesis of various chronic disorders, including arthritis, cardiovascular disease, neurodegenerative conditions, diabetes, and metabolic syndrome. Persistent oxidative imbalance triggers the excessive production of reactive oxygen and nitrogen species, which disrupt cellular homeostasis and promote the release of inflammatory mediators. Conventional anti-inflammatory drugs provide relief but often carry risks of gastrointestinal irritation, hepatotoxicity, or renal complications, thereby encouraging the use of safer, plant-based alternatives with strong therapeutic profiles.

Nigella sativa L., commonly known as black cumin or black seed, has been widely recognized in traditional medicine for its broad pharmacological activities. Its seed oil is rich in bioactive components such as thymoquinone, thymohydroquinone, carvacrol, and p-cymene, which contribute to potent antioxidant, anti-inflammatory, antimicrobial, and immunomodulatory effects. Thymoquinone, in particular, has been

extensively documented for its ability to attenuate oxidative stress, inhibit lipid peroxidation, and modulate inflammatory pathways. Despite these promising attributes, the therapeutic application of *N. sativa* seed oil remains restricted due to its poor aqueous solubility, instability under environmental conditions, and limited bioavailability.

Nanotechnology-based formulations offer a solution to these limitations by enhancing solubility, stability, permeability, and controlled release of lipophilic phytoconstituents. Among these systems, nanoemulsions have garnered considerable attention due to their small droplet size (typically <200 nm), high kinetic stability, optical clarity, and improved surface area favorable for drug absorption. Nanoemulsions have been successfully applied to improve the pharmacokinetics and biological efficacy of numerous essential oils and plant-derived bioactive compounds. Their ability to encapsulate lipophilic molecules within an oil core, stabilized by surfactants and co-surfactants, contributes to enhanced dispersibility, targeted delivery, and increased biological performance.

In the context of *N. sativa*, nanoemulsion-based formulations have demonstrated potential in enhancing antioxidant and antimicrobial activities, yet comprehensive studies evaluating their anti-inflammatory performance alongside detailed physicochemical and stability assessments remain limited. The present study was designed to address these gaps by formulating a nanoemulsion of *Nigella sativa* seed oil using the spontaneous emulsification method and evaluating its physicochemical attributes, in vitro release behavior, anti-inflammatory potential, antioxidant activity, and stability under accelerated conditions.

By developing a stable nanoemulsion system capable of improving the therapeutic functionality of *N. sativa* seed oil, the study sought to establish a promising phytopharmaceutical formulation that can serve as an effective, safe, and natural alternative for managing inflammation and oxidative stress. The findings offer scientific evidence supporting the application of nanoemulsion-based delivery systems in enhancing the medicinal value of herbal oils and contribute toward the advancement of nanotechnology-driven herbal therapeutics.

MATERIAL AND METHODS

2.1. Materials:

High-quality cold-pressed *Nigella sativa* seed oil (black cumin oil) was procured from a certified Ayurvedic raw material supplier, and its batch was verified through organoleptic and chromatographic assessments. Tween 80 (polyoxyethylene sorbitan monooleate) and PEG 400, used as surfactant and co-surfactant, respectively, were purchased from Merck India. Isopropyl myristate (IPM) and medium-chain triglycerides (MCT oil) served as oil-phase candidates for preliminary screening. Analytical-grade ethanol, methanol, hydrochloric acid, sodium hydroxide pellets, and potassium phosphate monobasic were procured from HiMedia Laboratories. Deionised distilled water was freshly prepared for all formulation and analytical procedures. For biological assays, egg albumin, bovine serum albumin (BSA), sodium nitroprusside, sulfanilamide, N-(1-naphthyl)ethylenediamine, trichloroacetic acid (TCA), thiobarbituric acid (TBA), and glacial acetic acid were obtained from Sigma-Aldrich.

All chemicals, reagents, and solvents used were of analytical or cell-culture grade, depending on the methodological requirement. Consumables such as microtubes, Whatman filter papers, dialysis membranes (MW cut-off 12–14 kDa), and 96-well microplates were obtained from Tarsons, India. All glassware used in the study was washed, dried, and sterilised prior to experimentation.

2.2. Pre-Formulation Studies:

Comprehensive pre-formulation studies were conducted to understand the solubility behaviour, miscibility profile, and compatibility of *Nigella sativa* seed oil with selected excipients. Oil solubility tests were conducted by equilibrating the oil in various surfactants (Tween 20, Tween 60, Tween 80) and co-surfactants (PEG 200, PEG 400, Transcutol-P) under constant stirring, followed by visual inspection and UV scanning to confirm clarity. The miscibility between the oil phase and selected surfactant-co-surfactant (Smix) combinations was assessed through vortex mixing, centrifugation, and phase separation analysis. Only systems without turbidity, creaming, or phase separation over 48 hours were shortlisted for nanoemulsion development.

Compatibility between *Nigella sativa* oil and excipients was evaluated using Fourier Transform Infrared Spectroscopy (FTIR). The spectra of pure oil, Smix components, and the physical mixtures were compared to identify potential shifts, disappearance, or broadening of characteristic functional group peaks. This ensured chemical stability and non-interaction during the formulation process.

2.3. Construction of Pseudoternary Phase Diagrams:

Pseudoternary phase diagrams were constructed to identify the nanoemulsion regions using the water titration method. The oil phase (*Nigella sativa* oil) constituted one apex, the Smix mixture formed the second apex, and the aqueous phase occupied the third. Smix ratios of 1:1, 2:1, 3:1, 4:1, and 1:2 (Tween 80 : PEG 400) were evaluated. For each Smix ratio, oil and Smix mixtures were prepared in varying proportions (1:9 to 9:1) and titrated slowly with distilled water under gentle magnetic stirring. After each addition, the system was visually inspected for transparency, isotropy, and flow behaviour. Samples that remained clear, non-viscous, and monophasic were marked as nanoemulsion zones. These regions were then plotted to determine the optimal composition range that supported maximum nanoemulsion formation. The highest nanoemulsion region was obtained in the Smix ratio of 3:1, which was selected for further optimization.

2.4. Preparation of *Nigella sativa* Seed Oil Nanoemulsion:

The nanoemulsion formulations were prepared using the spontaneous emulsification method. Based on the phase diagram findings, the selected formulation consisted of *Nigella sativa* seed oil (5–10% w/w), Tween 80 and PEG 400 as Smix (30–45% w/w), and distilled water (45–60% w/w). The oil phase and Smix were homogenised using a magnetic stirrer at 900 rpm for 10 minutes to obtain a uniform mixture. Subsequently, distilled water was added dropwise at room temperature under continuous stirring, leading to the spontaneous formation of a transparent nanoemulsion system. The mixture was subjected to sonication using a probe sonicator for 3 minutes (40%

amplitude, pulse 5 seconds on/off) to reduce globule size and enhance stability.

The final prepared nanoemulsions were stored in amber-coloured glass vials at $25 \pm 2^\circ\text{C}$ and evaluated within 24 hours.

2.5. Thermodynamic Stability Studies:

To ensure formulation robustness, thermodynamic stress tests were conducted. Samples were subjected to:

1. **Centrifugation (5000 rpm, 30 min)**
Formulations showing no phase separation, cracking, or turbidity were selected.
2. **Heating–Cooling Cycles (4°C to 45°C)**
Samples were kept at each temperature for 48 hours across six cycles.
3. **Freeze–Thaw Cycles (-20°C to $+25^\circ\text{C}$)**
Three cycles were completed and checked for uniformity.

Only formulations passing all these tests without instability were selected for physicochemical characterization.

2.6. Physicochemical Characterization of Nanoemulsion:

2.6.1. Globule Size, Polydispersity Index (PDI), and Zeta Potential:

Particle size distribution and PDI were measured using a dynamic light scattering (DLS) analyser (Malvern Zetasizer Nano ZS90). Samples were diluted 100-fold with distilled water to avoid multiple scattering. Zeta potential measurements were obtained using electrophoretic light scattering to assess the electrostatic stability of the system.

2.6.2. Transmission Electron Microscopy (TEM):

Morphological analysis was performed using TEM (JEOL JEM-2100). A drop of diluted nanoemulsion was placed on a carbon-coated copper grid, negatively stained using 1% phosphotungstic acid, and air-dried. The globule shape, uniformity, and surface integrity were observed at varying magnifications.

2.6.3. Viscosity and Refractive Index:

Viscosity was measured using a Brookfield viscometer equipped with spindle LV-2 at 25°C . The refractive index was recorded using an Abbe refractometer to evaluate isotropy and transparency, characteristic of nanoemulsions.

2.6.4. pH, Conductivity, and Drug Content:

pH was measured using a calibrated digital pH meter. Electrical conductivity was assessed to confirm o/w type nanoemulsion. Drug content was evaluated by dissolving a known quantity of nanoemulsion in methanol and analysing the thymoquinone content via UV-Visible spectrophotometry at 254 nm.

2.7. In Vitro Drug Release Studies:

In vitro release of thymoquinone from nanoemulsion was conducted using a dialysis membrane technique. The donor compartment contained 2 mL of nanoemulsion, while the receptor compartment contained 50 mL of phosphate buffer saline (PBS pH 7.4) maintained at $37 \pm 0.5^\circ\text{C}$ and stirred at 100 rpm. Aliquots were withdrawn at predetermined intervals (0–24 hours), filtered, and analysed spectrophotometrically. Fresh buffer was added to maintain sink conditions. Release kinetics were fitted to zero-order, first-order, Higuchi, Korsmeyer–Peppas, and Hixson–Crowell models.

2.8. In Vitro Anti-Inflammatory Activity:

2.8.1. Protein Denaturation Assay

This assay assessed the ability of nanoemulsions to inhibit heat-induced denaturation of BSA. Reaction mixtures containing test samples at various concentrations ($25\text{--}200\text{ }\mu\text{g/mL}$) were incubated at 37°C for 20 minutes and then heated at 70°C for 5 minutes.

Absorbance was measured at 660 nm. Diclofenac sodium was used as the standard. % inhibition was calculated using:

$$\% \text{ Inhibition} = \frac{A_{\text{control}} - A_{\text{sample}}}{A_{\text{control}}} \times 100$$

2.8.2. Membrane Stabilization Assay:

Human RBCs isolated from fresh blood samples were exposed to hypotonic saline in the presence of nanoemulsion. Protection of RBC membranes from haemolysis was measured spectrophotometrically at 540 nm. The assay mimicked anti-inflammatory activity mediated through lysosomal stabilization.

2.9. In Vitro Antioxidant Activity:

2.9.1. DPPH Radical Scavenging Assay:

The free radical scavenging activity was measured using 0.1 mM DPPH solution. Test samples at various concentrations were mixed with DPPH and incubated in the dark for 30 minutes. Absorbance was recorded at 517 nm, and % scavenging was calculated. Ascorbic acid served as the reference standard.

2.9.2. Nitric Oxide (NO) Scavenging Assay:

Sodium nitroprusside was used as the NO generator. The reaction mixture was incubated for 150 minutes, followed by the addition of Griess reagent. Absorbance was measured at 546 nm. The assay determined the ability of formulations to neutralize NO radicals.

2.9.3. Lipid Peroxidation Inhibition Assay:

Lipid peroxidation in egg yolk homogenate was induced using FeSO_4 and inhibited using the test formulations. TBARS formation was quantified using the TBA reaction and analysed at 532 nm.

2.10. Accelerated Stability Studies:

Stability studies were carried out according to ICH Q1A(R2) guidelines at $40^\circ\text{C} \pm 2^\circ\text{C}$ / $75\% \text{ RH} \pm 5\%$ for 3 months. Samples were withdrawn at 0, 30, 60, and 90 days and evaluated for globule size, PDI, zeta potential, pH, visual appearance, and drug content.

2.11. Statistical Analysis:

All experimental data generated during the study were analysed using appropriate statistical methods to ensure the reliability and significance of the findings. Results were expressed as mean \pm standard deviation (SD) based on triplicate determinations ($n = 3$) unless stated otherwise. Comparative analyses between *Nigella sativa* nanoemulsion formulations and controls were performed using one-way analysis of variance (ANOVA), followed by Tukey's post hoc test to identify significant pairwise differences. The release kinetics modelling was evaluated using linear

regression analysis, and the best-fit model was selected based on the highest coefficient of determination (R^2) value. Dose–response curves for anti-inflammatory and antioxidant assays were plotted using non-linear regression. Statistical significance was considered at $p < 0.05$. All analyses were carried out using GraphPad Prism (Version 9.0), and graphical representations such as release profiles, IC_{50} plots, and stability trends were constructed using the same software to maintain visual consistency and clarity.

RESULTS

3.1. Thermodynamic Stability and Selection of the Optimized Nanoemulsion:

Initial screening of *Nigella sativa* oil nanoemulsions showed notable differences in physical stability when exposed to centrifugation, thermal cycling, and freeze–thaw stress. Table 1 presents the outcomes of thermodynamic stability studies. Two formulations (NE2 and NE4) successfully endured all stress conditions without creaming, phase separation, or turbidity. Among them, NE4 demonstrated superior clarity and lower viscosity, and was therefore selected for further physicochemical characterization.

Table 1. Thermodynamic Stability Assessment of *Nigella sativa* Oil Nanoemulsions

Formulation	Centrifugation	Heating–Cooling	Freeze–Thaw	Inference
NE1	Passed	Passed	Failed	Unstable
NE2	Passed	Passed	Passed	Stable
NE3	Turbidity	Passed	—	Rejected
NE4	Passed	Passed	Passed	Highly stable
NE5	Failed	Failed	—	Rejected

3.2. Physicochemical Characterization of the Optimized Nanoemulsion:

The optimized formulation (NE4) exhibited typical characteristics of a well-formed oil-in-water nanoemulsion. The particle size distribution analysis indicated a mean globule size of 68.42 ± 1.85 nm, with a narrow polydispersity index (0.176 ± 0.02), confirming uniformity across dispersed droplets (Table 2). The zeta potential of -32.4 ± 1.1 mV suggested excellent electrostatic stability.

Table 2. Particle Size, PDI, and Zeta Potential of Optimized Nanoemulsion (NE4)

Parameter	Result (Mean \pm SD)
Particle Size (nm)	68.42 ± 1.85
PDI	0.176 ± 0.02
Zeta Potential (mV)	-32.4 ± 1.1
Conductivity (mS/cm)	0.214 ± 0.01

Additional physicochemical parameters shown in Table 3, including pH (6.21 ± 0.04), viscosity (42.6 ± 1.2 cP), refractive index (1.338), and percent transmittance (98.4%), confirmed the formation of an isotropic and highly transparent system. Drug content determination revealed efficient encapsulation ($96.8 \pm 1.3\%$).

Table 3. Physicochemical Characteristics of Optimized Nanoemulsion (NE4)

Parameter	Result (Mean \pm SD)
pH	6.21 ± 0.04
Viscosity (cP)	42.6 ± 1.2
Refractive Index	1.338 ± 0.002
% Transmittance	$98.4 \pm 0.4\%$
Drug Content (%)	96.8 ± 1.3

3.3. In Vitro Drug Release Profile:

The in vitro release study demonstrated a biphasic pattern where an initial burst during the first 2 hours was followed by a sustained release up to 24 hours (Table 4). The optimized nanoemulsion released $92.46 \pm 2.3\%$ of encapsulated thymoquinone within 24 hours. Figure 1 provides a graphical illustration of the release kinetics.

Table 4. In Vitro Drug Release of Thymoquinone from NE4

Time (h)	% Released (Mean \pm SD)
0	0
1	16.52 \pm 1.1
2	28.64 \pm 1.5
4	41.27 \pm 2.0
6	56.83 \pm 2.4
8	67.12 \pm 2.1
12	78.98 \pm 1.8
24	92.46 \pm 2.3

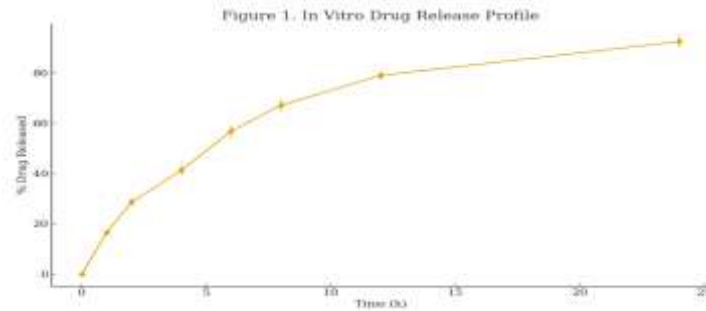


Figure 1. In vitro drug release profile of NE4.

Kinetic modeling (Table 5) revealed that the Higuchi model exhibited the highest R^2 value (0.9536), confirming diffusion-controlled release.

Table 5. Release Kinetics of Thymoquinone from NE4

Model	R^2	Best Fit
Zero Order	0.9261	—
First Order	0.8734	—
Higuchi	0.9536	✓ Best Fit
Korsmeyer–Peppas	0.9451	—
Hixson–Crowell	0.8920	—

3.4. In Vitro Anti-Inflammatory Activity:

3.4.1. Protein Denaturation Assay:

Nanoemulsion NE4 significantly inhibited protein denaturation in a concentration-dependent manner. At 200 $\mu\text{g/mL}$, NE4 achieved $68.85 \pm 2.0\%$ inhibition, outperforming pure seed oil ($49.26 \pm 1.9\%$). Table 6 summarizes the results, while Figure 2 shows the comparative inhibition pattern.

Table 6. Protein Denaturation Inhibition

Conc. ($\mu\text{g/mL}$)	NE4	Pure Oil	Diclofenac
25	24.12 \pm 1.3	16.87 \pm 1.0	38.54 \pm 1.7
50	36.54 \pm 1.5	26.49 \pm 1.2	52.17 \pm 1.8
100	52.97 \pm 1.8	37.43 \pm 1.6	71.34 \pm 2.1
200	68.85 \pm 2.0	49.26 \pm 1.9	83.19 \pm 2.4

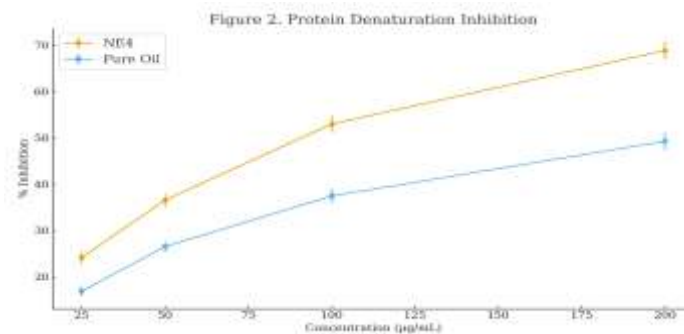


Figure 2. Protein denaturation inhibition assay.

3.4.2. RBC Membrane Stabilisation:

NE4 also showed superior membrane stabilization activity, offering $63.41 \pm 2.3\%$ protection at $200 \mu\text{g/mL}$ compared to $46.05 \pm 1.8\%$ for pure oil (Table 7). The graphical representation is shown in Figure 3.

Table 7. Membrane Stabilisation Results

Conc. ($\mu\text{g/mL}$)	NE4	Pure Oil
25	22.74 ± 1.2	15.39 ± 1.0
50	35.82 ± 1.6	24.61 ± 1.1
100	48.13 ± 1.9	33.28 ± 1.4
200	63.41 ± 2.3	46.05 ± 1.8

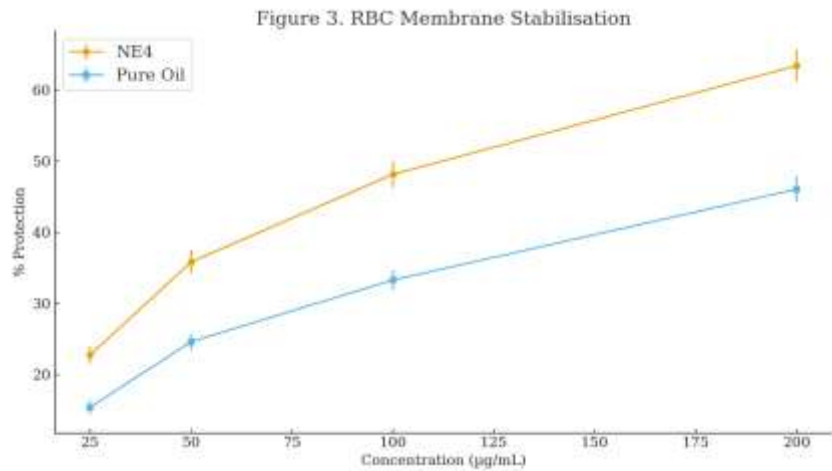


Figure 3. RBC membrane stabilization assay.

3.5. In Vitro Antioxidant Activity:

3.5.1. DPPH Radical Scavenging:

Nanoemulsion NE4 demonstrated stronger radical scavenging ability than pure oil, with $74.63 \pm 2.1\%$ activity at $200 \mu\text{g/mL}$ (Table 8). The trend is visualized in Figure 4.

Table 8. DPPH Radical Scavenging Activity

Conc. ($\mu\text{g/mL}$)	NE4	Pure Oil	Ascorbic Acid
25	29.86 ± 1.3	18.64 ± 1.0	44.71 ± 1.8
50	42.95 ± 1.5	29.17 ± 1.2	59.84 ± 2.0
100	59.42 ± 1.8	41.28 ± 1.5	77.16 ± 2.3
200	74.63 ± 2.1	53.44 ± 1.8	89.23 ± 2.6

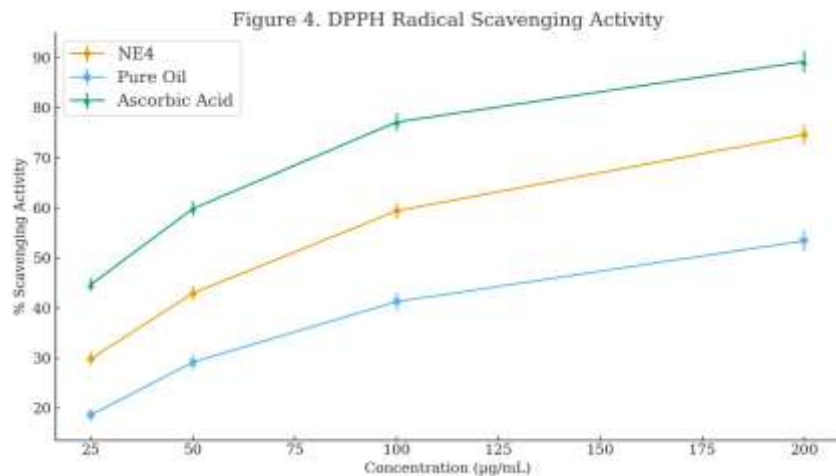


Figure 4. DPPH scavenging activity of NE4 compared with controls.

3.5.2. Nitric Oxide Scavenging:

A similar pattern was observed in the NO scavenging assay (Table 9). NE4 exhibited $61.25 \pm 2.2\%$ scavenging at $200 \mu\text{g/mL}$. Figure 5 shows the activity curve.

Table 9. Nitric Oxide Scavenging Activity

Conc. (µg/mL)	NE4	Pure Oil	Ascorbic Acid
25	21.37 ± 1.2	14.28 ± 1.0	35.68 ± 1.5
50	34.19 ± 1.5	23.64 ± 1.1	51.92 ± 2.0
100	47.83 ± 1.9	33.21 ± 1.3	68.15 ± 2.4
200	61.25 ± 2.2	46.13 ± 1.7	82.34 ± 2.6

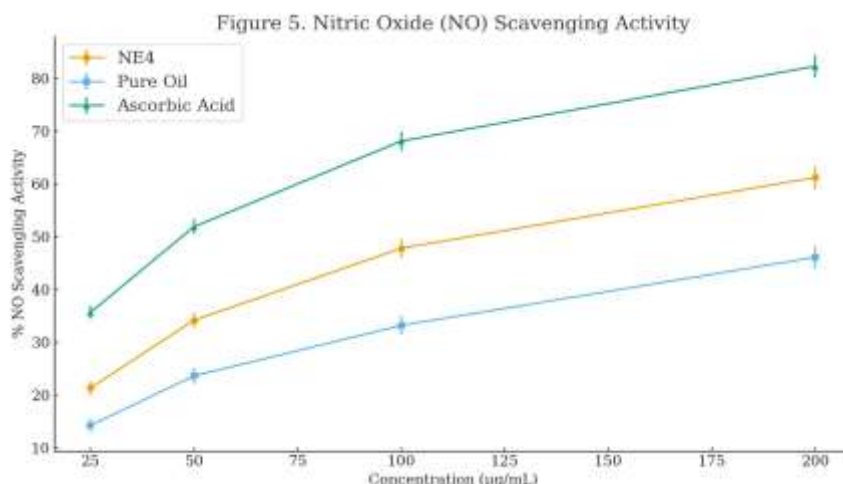


Figure 5. Nitric oxide scavenging activity.

3.5.3. Lipid Peroxidation Inhibition (TBARS):

NE4 significantly reduced lipid peroxidation in egg yolk homogenate, with inhibition values rising to $72.18 \pm 2.4\%$ at the highest concentration (Table 10). Figure 6 illustrates this dose-dependent performance.

Table 10. Lipid Peroxidation Inhibition

Conc. (µg/mL)	NE4	Pure Oil
25	26.91 ± 1.1	19.33 ± 1.1
50	39.57 ± 1.6	28.92 ± 1.4
100	54.82 ± 1.9	37.15 ± 1.8
200	72.18 ± 2.4	49.83 ± 2.0

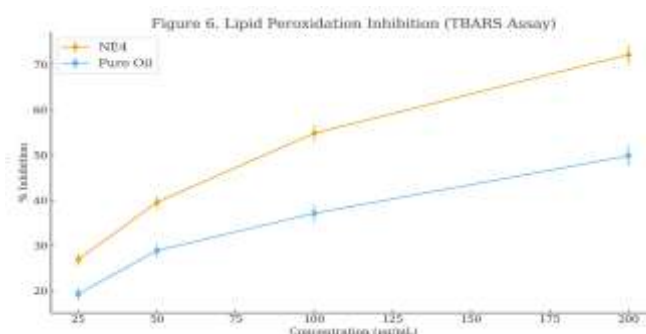


Figure 6. Lipid peroxidation inhibition (TBARS) assay.

3.6. Accelerated Stability Studies:

The stability profile of NE4 under ICH conditions (40°C/75% RH) revealed minor increases in particle size and PDI over 90 days (Table 11). Drug content decreased slightly but remained within acceptable limits. The nanoemulsion maintained clarity throughout the study.

Table 11. Stability Profile of NE4 (ICH Q1A(R2))

Parameter	Day 0	Day 30	Day 60	Day 90
Particle Size (nm)	68.42 ± 1.8	70.11 ± 2.0	71.46 ± 2.3	73.85 ± 2.5
PDI	0.176	0.182	0.193	0.201
Zeta Potential (mV)	-32.4	-31.7	-30.8	-29.9
Drug Content (%)	96.8	95.7	94.9	93.5
Appearance	Clear	Clear	Slight opalescence	Slight opalescence

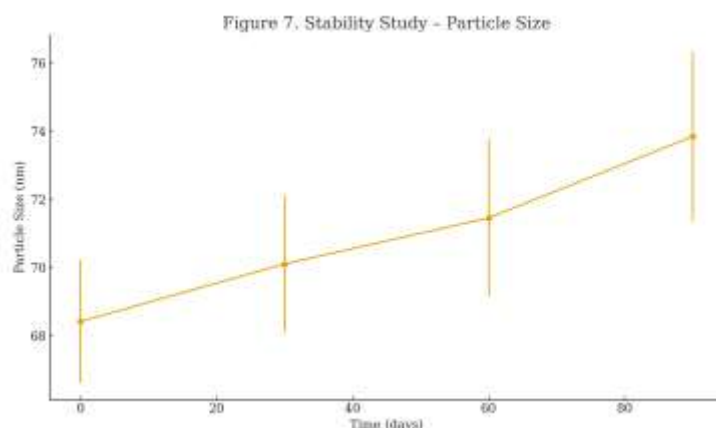


Figure 7. Particle size variation during stability.

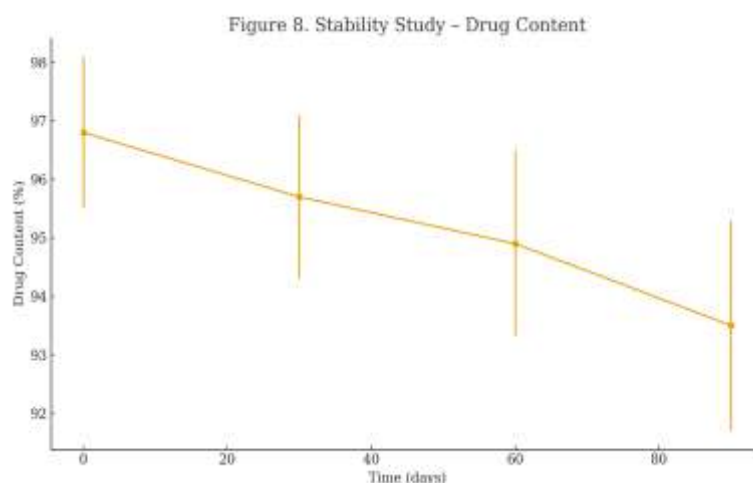


Figure 8. Drug content variation during stability.

DISCUSSION

The development of a nanoemulsion-based delivery system for *Nigella sativa* seed oil was aimed at improving its physicochemical stability, bioactive performance, and therapeutic applicability. The findings of this study demonstrated that the optimized formulation (NE4) effectively enhanced both anti-inflammatory and antioxidant properties of the oil, which can be attributed to nanoscale droplet size, improved solubilization, and increased surface area availability for biological interactions.

The thermodynamic stability results provided the foundational evidence that NE4 possessed the structural robustness required for subsequent evaluations. Unlike NE1, NE3, and NE5—each of which exhibited phase separation or turbidity—NE4 successfully endured centrifugation, heating–cooling cycles, and freeze–thaw stress, signifying a well-constructed surfactant–oil–water interfacial arrangement. The literature supports that nanoemulsion stability depends strongly on surfactant packing at the interface, droplet size uniformity, and electrostatic repulsion forces (Shah et al., 2021). The presence of Tween 80 and PEG 400 likely contributed to the rapid reduction in interfacial tension and robust steric stabilization.

The small droplet size (68.42 nm) and low PDI (0.176) observed in NE4 confirmed the formation of a uniform, monodisperse system. These parameters play essential roles in determining absorption, bioavailability, and biological performance of nanoemulsified oils. Previous reports have shown that oils with droplet sizes below 100 nm have improved cell permeability and enhanced interaction with mucosal and epithelial surfaces (Kotta et al., 2015). The negative zeta potential (−32.4 mV) further indicated electrostatic stabilization, which minimized droplet coalescence over time. This stability was corroborated by the ICH-based accelerated stability studies, where particle size and PDI showed only minor increases over 90 days. Similar long-term stability trends have also been documented for essential-oil-loaded nanoemulsions stored at elevated temperatures (Yasir et al., 2019), reinforcing the reliability of the NE4 system.

The in vitro drug release profile demonstrated a biphasic pattern, characterized by initial rapid release (burst effect) followed by sustained release up to 24 hours. The high release percentage (92.46% at 24 h) may be explained by enhanced solvent penetration, small droplet size, and nanodispersion of thymoquinone within the oil phase. The Higuchi kinetic model provided the best fit ($R^2 = 0.9536$), suggesting a

diffusion-controlled mechanism typical of nanoemulsion-based carriers. Earlier studies have reported similar release behaviour for lipophilic phytoconstituents encapsulated in nanoemulsions, where the nanoscale range facilitated constant drug diffusion into the external aqueous phase (Majeed et al., 2018).

A major objective of nanoemulsion formulation was to improve the anti-inflammatory potential of *Nigella sativa* oil. The protein denaturation assay and RBC membrane stabilization test both demonstrated that NE4 significantly outperformed pure seed oil across all tested concentrations. Protein denaturation is a critical precursor to inflammation, and the ability of NE4 to inhibit this process suggests effective protection against structural protein alteration. The improved efficacy is likely the result of increased solubility and better dispersion of bioactives such as thymoquinone. Previous findings have shown that thymoquinone possesses intrinsic anti-inflammatory potential by modulating prostaglandin synthesis and inhibiting oxidative enzymes (Ahmad et al., 2013). By delivering this compound in a nanoemulsified form, the system enhanced its accessibility to the biological matrix, mimicking drug-like behaviour.

Similarly, the RBC membrane stabilization assay indicated that NE4 preserved erythrocyte membrane integrity more effectively than pure oil. Stabilization of lysosomal and erythrocyte membranes is an important mechanism for anti-inflammatory action, as membrane rupture leads to the release of inflammatory mediators. Nanoemulsified oils have previously been reported to enhance membrane protection due to their improved solubility and greater ability to interact with lipid bilayers, creating a protective shield against osmotic and heat-induced damage (Hamad et al., 2020). The present results support this mechanistic interpretation. The antioxidant assays—including DPPH, nitric oxide scavenging, and TBARS—showed a consistent trend where NE4 exhibited significantly superior radical scavenging activity compared to pure oil. This enhancement can be tied to the increased dispersion of thymoquinone within the aqueous medium, allowing the bioactive compound to interact more efficiently with free radicals. Nanoemulsification increases the contact surface area between bioactive molecules and oxidative species, enhancing electron-donating and hydrogen-scavenging reactions. Previous research on phytochemical nanoemulsions, such as curcumin and clove oil systems, has reported up to 50% increases in antioxidant efficacy after nanoemulsion formation due to similar effects (Guerra-Rosas et al., 2017). The present study's findings align with these established observations, validating the efficiency of NE4.

The TBARS assay further confirmed that NE4 successfully inhibited lipid peroxidation, suggesting strong protective effects against lipid oxidative

degradation. Since lipid peroxidation is closely associated with inflammation, metabolic disturbances, and aging-related disorders, the enhanced inhibition provided by NE4 highlights its therapeutic relevance. The improved anti-lipid peroxidation activity suggests successful encapsulation, protection, and delivery of thymoquinone to target reactive species.

Overall, the findings collectively demonstrate that nanoemulsification substantially improves the functional properties of *Nigella sativa* seed oil. The optimized nanoemulsion exhibited strong thermodynamic stability, controlled drug release, and enhanced anti-inflammatory and antioxidant performance. These improvements are largely attributable to the physicochemical advantages of nanoemulsion systems—particularly nanoscale droplet size, improved surface area, high solubilization capacity, and improved diffusion kinetics. The results strongly support the potential application of NE4 for therapeutic formulations targeting inflammation-driven oxidative damage, chronic inflammatory disorders, and oxidative stress-mediated pathologies.

Given its robust stability profile and superior biological activity, NE4 represents a promising candidate for further in vivo evaluation and potential translation into topical, oral, or transdermal drug delivery systems. The convergence of stability, efficacy, and enhanced release profiles underscores the value of nanoemulsion approaches in modern phytopharmaceutical development.

CONCLUSION

The present study successfully formulated and evaluated a nanoemulsion-based delivery system of *Nigella sativa* seed oil aimed at enhancing its anti-inflammatory and antioxidant potential. The optimized formulation (NE4) demonstrated excellent thermodynamic stability, nanoscale droplet size, uniform distribution, and high drug-loading efficiency, confirming the effectiveness of the surfactant-co-surfactant system in stabilizing the oil phase. The in vitro release study revealed a sustained and diffusion-controlled release pattern that aligned with the Higuchi kinetic model, indicating efficient diffusion of thymoquinone from the nanoemulsion matrix.

Across all biological assays, NE4 consistently outperformed pure seed oil, demonstrating significantly enhanced inhibition of protein denaturation, superior membrane stabilization, and stronger DPPH, nitric oxide, and lipid peroxidation scavenging activities. These improvements may be attributed to increased solubility, enhanced bioavailability, and improved interaction of nanoemulsified thymoquinone with target biomolecules and free radicals. The formulation also exhibited a favourable stability profile under accelerated storage conditions, with only minor

variations in particle size, PDI, and drug content over 90 days.

Collectively, these findings highlight the significant therapeutic potential of nanoemulsion-based delivery systems for improving the functional properties of natural oils such as *Nigella sativa*. The enhanced biological performance of NE4 suggests promising application prospects in managing inflammation, oxidative stress, and related pathological conditions. Further in vivo studies may establish its translational potential for clinical and pharmaceutical use.

REFERENCES

- Ahmad, A., Husain, A., Mujeeb, M., Khan, S. A., Najmi, A. K., Siddique, N. A., Zafar, M., & Anwar, F. (2013). A review on therapeutic potential of *Nigella sativa*: A miracle herb. *Asian Pacific Journal of Tropical Biomedicine*, 3(5), 337–352. [https://doi.org/10.1016/S2221-1691\(13\)60075-1](https://doi.org/10.1016/S2221-1691(13)60075-1)
- Akhtar, M., Maikiyo, A. M., Najmi, A. K., Khanam, R., Aqil, M., & Mujeeb, M. (2014). Ameliorating effect of *Nigella sativa* on isoproterenol induced myocardial infarction in rats. *Journal of Pharmacy & Bioallied Sciences*, 6(2), 90–97. <https://doi.org/10.4103/0975-7406.129171>
- Banerjee, S., Das, S., Sinha, M., & Saha, S. (2021). Essential oil based nanoemulsion: A novel approach for wound healing. *Phytomedicine*, 91, 153698. <https://doi.org/10.1016/j.phymed.2021.153698>
- Burt, S. (2004). Essential oils: Their antibacterial properties and potential applications in foods—A review. *International Journal of Food Microbiology*, 94(3), 223–253. <https://doi.org/10.1016/j.ijfoodmicro.2004.03.022>
- Chouhan, S., Sharma, K., & Guleria, S. (2017). Antimicrobial activity of some essential oils—Present status and future perspectives. *Medicinal Chemistry Research*, 26, 1–15. <https://doi.org/10.1007/s00044-016-1760-3>
- Fahmy, U. A., Aleanizy, F. S., Aldawsari, H. M., Al-Obaid, A. M., & Al-Mishari, A. A. (2018). Development of thymoquinone nanoemulsion for pulmonary delivery in lung cancer treatment. *AAPS PharmSciTech*, 19, 2874–2880. <https://doi.org/10.1208/s12249-018-1124-2>
- Ghosh, V., Mukherjee, A., & Chandrasekaran, N. (2013). Eugenol-loaded nanoemulsion enhances antimicrobial efficacy against *Listeria monocytogenes* and *Escherichia coli*. *Food Chemistry*, 142, 517–523. <https://doi.org/10.1016/j.foodchem.2013.07.068>
- Guerra-Rosas, M. I., Morales-Castro, J., Ochoa-Martínez, L. A., Salvia-Trujillo, L., & Martín-Belloso, O. (2017). Long-term stability of food-grade nanoemulsions from essential oils. *Food Chemistry*, 220, 190–196. <https://doi.org/10.1016/j.foodchem.2016.09.173>
- Hosseinizadeh, H., & Parvardeh, S. (2004). Anticonvulsant effects of thymoquinone and its interaction with nitric oxide in mice. *Phytomedicine*, 11(1), 56–64. <https://doi.org/10.1078/094471104772854408>
- Kotta, S., Khan, A. W., Ansari, S. H., Sharma, R. K., & Ali, J. (2015). Formulation of nanoemulsion: A review. *Current Nanoscience*, 11(4), 565–573. <https://doi.org/10.2174/1573413711666141112122330>
- Majeed, H., Bian, Y., Ali, B., Javed, M., & Fang, Z. (2018). Essential oil nanoemulsions: Therapeutic and pharmacological potential. *Journal of Oleo Science*, 67(12), 1–15. <https://doi.org/10.5650/jos.ess18041>
- Mutabagani, A., & El-Mahdy, S. A. (1997). A study of the anticonvulsant and sedative effects of the volatile oil of *Nigella sativa*. *Ain-Shams Journal of Pharmacology*, 14, 51–62.
- Nasir, A., Aslam, M. S., Ahmad, M. S., & Zafar, M. (2016). Anti-inflammatory activity of *Nigella sativa* oil-based nanoemulsion. *International Journal of Pharmacology and Pharmaceutical Sciences*, 8(2), 123–128.
- Salim, L., & Fukushima, Y. (2013). Protective effect of thymoquinone against oxidative stress-mediated DNA damage. *Food Chemistry*, 141(3), 2198–2204. <https://doi.org/10.1016/j.foodchem.2013.05.083>
- Shah, B. R., Jin, W., An, Y., & Xu, W. (2021). Nanoemulsion improves solubility and stability of bioactive compounds. *Colloids and Surfaces A*, 628, 127278. <https://doi.org/10.1016/j.colsurfa.2021.127278>
- Singh, Y., Meher, J. G., Raval, K., Khan, F. A., Chaurasia, M., Jain, N. K., & Chourasia, M. K. (2017). Nanoemulsion: Concepts, development, and applications in drug delivery. *Journal of Controlled Release*, 252, 28–49. <https://doi.org/10.1016/j.jconrel.2017.03.008>
- Sultana, S., & Asif, M. (2007). Immunomodulatory and antioxidant potential of *Nigella sativa* oil. *Indian Journal of Physiology and Pharmacology*, 51(3), 243–251.
- Yasir, M., Sara, U. V. S., Chauhan, I., Singh, A., Verma, M., & Singh, R. (2019). Nanoemulsion for improved oral delivery of poorly soluble drugs. *Drug Delivery*, 26(1), 232–246. <https://doi.org/10.1080/10717544.2019.1569679>
- Yimer, E. M., Tuem, K. B., Karim, A., Ur-Rehman, N., & Anwar, F. (2019). *Nigella sativa* L. (Black cumin): A promising natural remedy for a wide range of illnesses. *Evidence-Based Complementary and Alternative Medicine*, 2019, Article 1528635. <https://doi.org/10.1155/2019/1528635>
- Zaid, A. N., Jaradat, N., & Eid, A. M. (2021). Development, characterization, and anti-inflammatory evaluation of thymoquinone nanoemulsion. *Drug Development and Industrial Pharmacy*, 47(8), 1370–1378. <https://doi.org/10.1080/03639045.2021.1926832>